

Graph-Conditioned MLP for High-Dimensional Tabular Biomedical Data

Andrei Margeloiu¹ Nikola Simidjievski¹ Pietro Lió¹ Mateja Jamnik¹

Introduction

Genome-wide studies leveraging recent high-throughput sequencing technologies aim to better understand human diseases and facilitate adequate treatments through personalised medicine. Such studies collect high-dimensional biomedical data but usually include small cohorts of patients. The resulting tabular biomedical datasets typically suffer from the “curse of dimensionality”, as the number of features is much larger than the number of samples ($D \gg N$). Even though well-regularised MLPs surpass specialised neural networks on tabular datasets [7], they are unstable to train and overfit when the datasets are small-size and high-dimensional.

We seek to address two problems of MLPs applied to such datasets. Firstly, MLPs applied to high-dimensional data contain a disproportionate number of parameters in the first layer. For example, on a typical genomics dataset with $\sim 20,000$ features, a five-layer MLP with 100 neurons per layer contains 98% of the parameters in the first layer, and can lead to overfitting. Secondly, training MLPs on small-size datasets is cumbersome because modern initialisation strategies [4, 5] put ‘weak priors’ on the model’s parameters. For instance, they assume independence between a layer’s weights and independence between a layer’s activations. Such simplistic assumptions are suitable for large datasets because they allow flexibility but are unsuitable when there are not enough samples to estimate the model’s parameters robustly. We hypothesise that more robust priors on the parameters would alleviate both issues.

We propose **Graph-Conditioned MLP (GC-MLP)**, a novel method to introduce priors on the parameters of an MLP. Instead of initialising the first layer $\mathbf{W}^{[1]}$ at random, we seek to condition it directly on the training data \mathbf{X} according to $\mathbf{W}^{[1]}|\mathbf{X}$. More specifically, we create a graph for each feature in the dataset (e.g., a gene), where each node represents a sample from the same dataset (e.g., a patient). In turn, we use Graph Neural Networks (GNNs) to learn embeddings from these graphs, which we then use to initialise $\mathbf{W}^{[1]}$.

¹Department of Computer Science and Technology, University of Cambridge, UK. Correspondence to: <am2770@cam.ac.uk>.

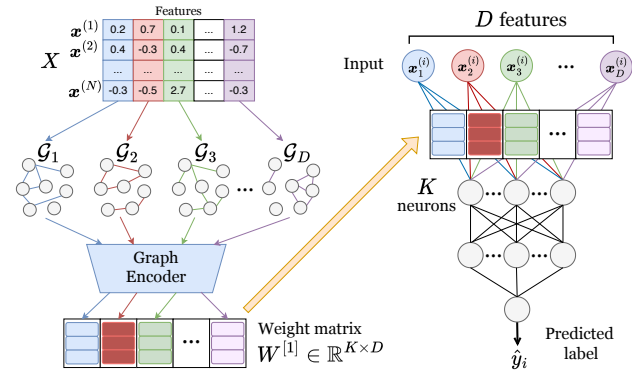


Figure 1. Overview of proposed method **GC-MLP**. Given a tabular dataset \mathbf{X} , we create a graph \mathcal{G}_j for each feature j . From each graph \mathcal{G}_j we extract graph embeddings $\mathbf{w}^{(j)}$ and concatenate them horizontally. The results matrix $\mathbf{W}^{[1]}$ is used to initialise the first layer of a standard MLP applied on the tabular dataset \mathbf{X} .

One benefit of our approach is conditioning the MLP’s parameters on the graphs, thus opening the prospect of introducing additional biological knowledge when constructing the graphs. We present early results on 7 classification tasks from gene expression data (in real applications, this could mean identifying biomarkers for different diseases) and show that GC-MLP outperforms an MLP. Lastly, we discuss extending this method to provide model explanations.

Method

Figure 1 illustrates the proposed method. We define the data matrix as $\mathbf{X} \in \mathbb{R}^{N \times D}$ and create D graphs from it. Specifically, for each feature j we use its values $X_{:,j}$ to construct an undirected graph $\mathcal{G}_j = (\mathcal{V}, \mathcal{E}_j)$. The nodes in each graph \mathcal{V} represent the data samples (in our experiments – patients) with node-features as a one-hot vector. To this end, in our experiments we use a simple heuristic to create edges: connecting nodes with similar feature values. Namely, nodes k and l are connected in the graph \mathcal{G}_j if $(|X_{k,j} - X_{l,j}| < 0.05 * (\max(X_{:,j}) - \min(X_{:,j})))$. We connect each node with at most 25 closest neighbours.

GC-MLP acts as an initialisation scheme for the first layer, and training this method includes two steps. Firstly, we compute graph embeddings for each graph using a Graph Autoencoder (GAE) [9] with a Graph Convolutional Network GCN [10] backbone. Let \mathbf{A}_j be the adjacency ma-

Table 1. Comparing the proposed method GC-MLP against an MLP on 7 biomedical datasets. We report the mean and standard deviation of the balanced accuracy on the test set, averaged across 25 runs. We **bold** the highest accuracy for each dataset.

	metabric-dr	metabric-pam50	smk	tcga-2y-survival	tcga-tumor-grade	lung	toxicity
DietNetworks [16]	56.98 ± 8.70	95.02 ± 4.77	62.71 ± 9.38	53.62 ± 5.46	46.69 ± 7.11	90.43 ± 6.23	82.13 ± 7.42
FsNet [18]	56.92 ± 10.13	83.86 ± 8.16	56.27 ± 9.23	53.83 ± 7.94	45.94 ± 9.80	91.75 ± 3.04	60.26 ± 8.10
MLP	58.6 ± 7.9	95.94 ± 3.83	61.5 ± 9.54	55.17 ± 7.98	50.53 ± 11.59	95.04 ± 5.03	92.72 ± 4.7
GC-MLP	60.26 ± 8.69	96.73 ± 3.69	62.42 ± 6.79	56.16 ± 7.9	51.1 ± 9.82	95.18 ± 4.59	92.51 ± 5.1
GC-MLP (joint training)	55.26 ± 8.36	92.47 ± 8.17	56.33 ± 8.20	52.25 ± 7.59	48.32 ± 12.22	90.07 ± 7.54	69.31 ± 8.15

trix for graph \mathcal{G}_j . For each graph \mathcal{G}_j , the GAE computes node embeddings $\mathbf{Z}_j = \text{GCN}(\mathbf{I}_N, \mathbf{A}_j)$ and then reconstructs the adjacency matrix $\hat{\mathbf{A}}_j = \sigma(\mathbf{Z}_j \mathbf{Z}_j^\top)$. The GAE’s objective is to minimise the negative log-likelihood of reconstructing the adjacency matrix. We compute D graph embeddings $\mathbf{w}^{(j)}$ by applying global average pooling on the node embeddings of each graph. The graph embeddings are concatenated horizontally to obtain the weight matrix $\mathbf{W}^{[1]} = [\mathbf{w}^{(1)}, \mathbf{w}^{(2)}, \dots, \mathbf{w}^{(D)}] \in \mathbb{R}^{K \times D}$, where K is the number of neurons on the first layer. Secondly, the MLP is trained as usual to minimise the cross-entropy loss.

What is the inductive bias of this method? Intuitively, GC-MLP pre-initialises the features learned by neurons in the first layer of the MLP. The GAE extracts latent features from the graphs, such that $\mathbf{W}_{ij}^{[1]}$ represents ‘how present’ is the learned latent feature i in the graph \mathcal{G}_j . Consequently, we use the values of the k -th latent feature across all graphs to initialise the weights connecting the k -th neuron with all input features (i.e., $\mathbf{W}_{k,:}^{[1]}$). In the beginning, the first layer’s neurons will ignore the features where some latent features are not present (i.e., the weight $\mathbf{W}_{ij}^{[1]} \approx 0$).

Why is this method particularly suitable for high-dimensional and small-size datasets? On the one hand, the problem’s high-dimensionality leads to many graphs, which serve as a large training set for the GAE. On the other hand, the computation is efficient since the graphs are very small as the number of samples N is small.

Experiments

We evaluate the method on 7 classification tasks using real-world gene expression datasets. These datasets contain between 3312–19993 features, between 111–200 samples, and between 2–4 classes (details in Appendix A). For each dataset, we perform 5-fold cross-validation repeated 5 times, resulting in 25 runs per model. We randomly select 10% of the training data for validation for each fold. As a benchmark, we consider an MLP with hidden layers of size 100, 100, 10 and softmax activation. The MLP and GC-MLP use the same architecture. The graphs are computed from the training data only. We train the MLP and GC-MLP with weighted cross-entropy loss. Appendix B contains complete training details.

We consider two modes of training GC-MLPs: A two-step and an end-to-end mode. In the former, we first train the autoencoder independently from the MLP, and subsequently initialise the MLP with learnt graph embeddings. In the latter, motivated by previous work on parameter prediction [16, 18], we considered an end-to-end version of our method, called **GC-MLP (joint training)** in Table 1. The weight matrix $\mathbf{W}^{[1]}$ is computed using the GAE at every iteration. Accordingly, the first layer of the MLP acts as a ‘virtual layer’ because the weights $\mathbf{W}^{[1]}$ are computed by the GAE rather than learned directly (which reduces the number of learnable parameters by $\sim 90\%$). This approach jointly trains the GAE and the MLP to minimise the cross-entropy loss using back-propagation.

Results Table 1 compares the two variants of GC-MLP against an MLP baseline. We observe that GC-MLP outperforms an MLP on 6 out of 7 datasets, except ‘toxicity’, on which it performs similarly. Also, on 5 out of 7 datasets GC-MLP has a smaller standard deviation, and we hypothesise that it could potentially alleviate the MLP’s training instabilities. We find these preliminary results encouraging. However, our early results of the jointly trained variant show that this approach is less successful than the vanilla MLP.

Discussion

One of the key advantages of our approach is that using graphs opens the possibility to further condition the model using biological knowledge, for example, using protein-protein interaction (PPI) networks to guide the construction of predictive models [17]. Although the two-step GC-MLP approach for initialising MLPs showed good empirical results, we see potential in further investigating joint training of GC-MLP. The end-to-end nature of the model could provide valuable interpretability insights. From a medical perspective, this approach could provide explanations using a cohort of similar patients (e.g., by finding suitable patient subgraphs) or concept-based explanations for GNNs [14, 15]. Such model explanations could be helpful in the pursuit of discovering new biological insights. From a machine learning perspective, GC-MLP may provide new insights into the data, allowing outliers detection, detecting mislabeled samples, or finding the influential training points.

References

- [1] Gagan Bajwa, Ralph J DeBerardinis, Baomei Shao, Brian Hall, J David Farrar, and Michelle A Gill. Cutting edge: Critical role of glycolysis in human plasmacytoid dendritic cell antiviral responses. *The Journal of Immunology*, 196(5):2004–2009, 2016.
- [2] Arindam Bhattacharjee, William G Richards, Jane Staunton, Cheng Li, Stefano Monti, Priya Vasa, Christine Ladd, Javad Beheshti, Raphael Bueno, Michael Gillette, et al. Classification of human lung carcinomas by mrna expression profiling reveals distinct adenocarcinoma subclasses. *Proceedings of the National Academy of Sciences*, 98(24):13790–13795, 2001.
- [3] Christina Curtis, Sohrab P Shah, Suet-Feung Chin, Gulisa Turashvili, Oscar M Rueda, Mark J Dunning, Doug Speed, Andy G Lynch, Shamith Samarajiwa, Yinyin Yuan, et al. The genomic and transcriptomic architecture of 2,000 breast tumours reveals novel subgroups. *Nature*, 486(7403):346–352, 2012.
- [4] Xavier Glorot and Yoshua Bengio. Understanding the difficulty of training deep feedforward neural networks. In *Proceedings of the thirteenth international conference on artificial intelligence and statistics*, pages 249–256. JMLR Workshop and Conference Proceedings, 2010.
- [5] Kaiming He, Xiangyu Zhang, Shaoqing Ren, and Jian Sun. Delving deep into rectifiers: Surpassing human-level performance on imagenet classification. In *Proceedings of the IEEE international conference on computer vision*, pages 1026–1034, 2015.
- [6] Sergey Ioffe and Christian Szegedy. Batch normalization: Accelerating deep network training by reducing internal covariate shift. In *International Conference on Machine Learning*, pages 448–456. PMLR, 2015.
- [7] Arindam Kadra, Marius Lindauer, Frank Hutter, and Josif Grabocka. Well-tuned simple nets excel on tabular datasets. *Advances in Neural Information Processing Systems*, 34, 2021.
- [8] Diederik P. Kingma and Jimmy Ba. Adam: A method for stochastic optimization. *International Conference on Learning Representations*, 2015.
- [9] Thomas Kipf and Max Welling. Variational graph auto-encoders. *NeurIPS Bayesian Deep Learning Workshop*, 2016.
- [10] Thomas Kipf and Max Welling. Semi-supervised classification with graph convolutional networks. *International Conference on Learning Representations*, 2017.
- [11] Jundong Li, Kewei Cheng, Suhang Wang, Fred Morstatter, Robert P Trevino, Jiliang Tang, and Huan Liu. Feature selection: A data perspective. *ACM Computing Surveys (CSUR)*, 50(6):94, 2018.
- [12] Arthur Liberzon, Chet Birger, Helga Thorvaldsdóttir, Mahmoud Ghandi, Jill P Mesirov, and Pablo Tamayo. The molecular signatures database hallmark gene set collection. *Cell systems*, 1(6):417–425, 2015.
- [13] Ilya Loshchilov and Frank Hutter. Decoupled weight decay regularization. In *International Conference on Learning Representations*, 2019.
- [14] Lucie Charlotte Magister, Pietro Barbiero, Dmitry Kazhdan, Federico Siciliano, Gabriele Ciravegna, Fabrizio Silvestri, Mateja Jamnik, and Pietro Lio. Encoding concepts in graph neural networks. *arXiv preprint arXiv:2207.13586*, 2022.
- [15] Lucie Charlotte Magister, Dmitry Kazhdan, Vikash Singh, and Pietro Lio. Gcexplainer: Human-in-the-loop concept-based explanations for graph neural networks. *ICML Workshop on Human in the Loop Learning*, 2021.
- [16] Adriana Romero, Pierre Luc Carrier, Akram Erraqabi, Tristan Sylvain, Alex Auvolet, Etienne Dejoie, Marc-André Legault, Marie-Pierre Dubé, Julie G. Hussin, and Yoshua Bengio. Diet networks: Thin parameters for fat genomics. In *International Conference on Learning Representations*, 2017.
- [17] Paul Scherer, Maja Trebacz, Nikola Simidjievski, Ramon Viñas, Zohreh Shams, Helena Andres Terre, Mateja Jamnik, and Pietro Lio. Unsupervised construction of computational graphs for gene expression data with explicit structural inductive biases. *Bioinformatics*, 38(5):1320–1327, 2022.
- [18] Dinesh Singh, Héctor Climente-González, Mathis Petrovich, Eiryō Kawakami, and Makoto Yamada. Fsnnet: Feature selection network on high-dimensional biological data. *arXiv preprint arXiv:2001.08322*, 2020.
- [19] Avrum Spira, Jennifer E Beane, Vishal Shah, Katrina Steiling, Gang Liu, Frank Schembri, Sean Gilman, Yves-Martine Dumas, Paul Calner, Paola Sebastiani, et al. Airway epithelial gene expression in the diagnostic evaluation of smokers with suspect lung cancer. *Nature medicine*, 13(3):361–366, 2007.
- [20] Nitish Srivastava, Geoffrey Hinton, Alex Krizhevsky, Ilya Sutskever, and Ruslan Salakhutdinov. Dropout: a simple way to prevent neural networks from overfitting. *The journal of machine learning research*, 15(1):1929–1958, 2014.
- [21] Katarzyna Tomczak, Patrycja Czerwińska, and Maciej Wiznerowicz. The cancer genome atlas (tcga): an immeasurable source of knowledge. *Contemporary oncology*, 19(1A):A68, 2015.

A. Datasets

Table 2. Details of the 7 real-world biomedical datasets used for experiments. The number of features is 15 – 110 times larger than the number of samples.

Dataset	# Samples	# Features	# Classes	# Samples per class
lung	197	3312	4	17, 20, 21, 139
metabric-dr	200	4160	2	61, 139
metabric-pam50	200	4160	2	33, 167
smk	187	19993	2	90, 97
tcga-2ysurvival	200	4381	2	78, 122
tcga-tumor-grade	200	4381	3	25, 52, 124
toxicity	171	5748	4	39, 42, 45, 45

All datasets are publicly available, and summarised in Table 2. Three datasets [11] and available online (<https://jundongl.github.io/scikit-feature/datasets.html>): **lung** [2], **SMK-CAN-187** (called ‘smk’) [19] and **TOX-171** (called ‘toxicity’) [1].

We derived two datasets from the **METABRIC** [3] dataset. We combined the molecular data with the clinical label ‘DR’ to create the ‘**metabric-dr**’ dataset, and we combined the molecular data with the clinical label ‘Pam50Subtype’ to create the ‘**metabric-pam50**’ dataset. Because the label ‘Pam50Subtype’ was very imbalanced, we transformed the task into a binary task of basal vs non-basal by combining the classes ‘LumA’, ‘LumB’, ‘Her2’, ‘Normal’ into one class and using the remaining class ‘Basal’ as the second class. For both ‘metabric-dr’ and ‘metabric-pam50’ we selected the Hallmark gene set [12] associated with breast cancer, and the new datasets contain 4160 expressions (features) for each patient. We created the final datasets by randomly sampling 200 patients stratified because we are interested in studying datasets with a small sample size.

We derived two datasets from the **TCGA** [21] dataset. We combined the molecular data and the label ‘X2yr.RF.Surv’ to create the ‘**tcga-2ysurvival**’ dataset, and we combined the molecular data and the label ‘tumor_grade’ to create the ‘**tcga-tumor-grade**’ dataset. For both ‘tcga-2ysurvival’ and ‘tcga-tumor-grade’ we selected the Hallmark gene set [12] associated with breast cancer, leaving 4381 expressions (features) for each patient. We created the final datasets by randomly sampling 200 patients stratified because we are interested in studying datasets with a small sample size.

Dataset processing Before training the models, we apply Z-score normalisation to each dataset. Specifically, on the training split, we learn a simple transformation to make each column of $\mathbf{X}_{train} \in \mathbb{R}^{N_{train} \times D}$ have zero mean and unit variance. We apply this transformation to the validation and test splits during cross-validation.

B. Training details

We performed hyper-parameter tuning for all models and all datasets, and selected the best settings on the validation loss.

For **MLP** and **GC-MLP** we train for 10,000 iterations using early stopping with patience 200 on the validation cross-entropy. We use gradient clipping at 2.5, batch normalisation [6], dropout [20] with $p = 0.2$ and LeakyReLU nonlinearity internally. We train with a batch size of 8 and optimise using AdamW [13] with a learning rate $3e - 3$ and weight decay of $1e - 4$. We use a learning-rate scheduler, linearly decaying the learning rate from $3e - 3$ to $3e - 4$ over 500 epochs, and continue training with $3e - 4$.

For **DietNetworks** [16] we used the same architecture and training schedule as for the MLP. On all datasets, DietNetworks performed best without a decoder. We used the feature embeddings suggested in [18] with 50 bins.

For **FsNet** [18] we used the same architecture as for the MLP. We used the feature embeddings suggested in [18] with 50 bins. We used the suggested annealing schedule for the concrete nodes: exponential annealing from temperature 10 to 0.01. We use the same training procedure as for the MLP, but with different learning rates. On ‘toxicity’ the learning rate starts at 0.001, and the λ for reconstruction is 0.2. On ‘lung’ the learning rate starts at 0.001 and λ for reconstruction is 0. On all other datasets we train with learning rate starts at 0.003 and λ for reconstruction is 0.

The **GAE** has two GCN layers with a hidden size of 40 and dropout with $p = 0.5$. We create negative edges in equal number to the positive edges. The GAE is trained for 1000 iterations using Adam [8] with learning rate 0.001 and batch size 8.